IRANIAN JOURNAL OF BOTANY 31(2), 2025
DOI: https://doi.org/10.22092/ijb.2025.369441.1523

PHYLOGENY AND SPECIES DELIMITATION IN THE MEDICAGO RIGIDULA (L.) ALL. COMPLEX BASED ON nrDNA SEQUENCE DATA

Zahra Ghorbani[1], Iraj Mehregan[2*], Mostafa Assadi[3], Ernest Small[4]

[1]*Department of Plant Sciences, Faculty of Biological Sciences, Kharazmi University, Tehran, Iran.*
[2]*Department of Biology, SR.C., Islamic Azad University, Tehran, Iran.*
[3]*Research Institute of Forests and Rangelands, Agricultural Research Education and Extension Organization (AREEO)*
[4] *Biosystematics Research Institute, Agriculture Canada, K1A OC6, Ottawa, Ontario, Canada.*
corresponding author: Iraj Mehregan, imehregan@srbiau.ac.ir; iraj@daad-alumni.de

Citation: Ghorbani, Z., Mehregan, I., Assadi, M., Small, E. 2025: Phylogeny and species delimitation in the *Medicago rigidula* (L.) All. complex based on the nrDNA sequence data. - Iran. J. Bot. 31(2): 177-193. https://doi.org/10.22092/ijb.2025.369441.1523

Article history
Received: 11 May 2025
Revised: 24 September 2025
Accepted: 07 November 2025
Published: 30 December 2025

Abstract
Annual species of the genus *Medicago* L. (Fabaceae) are ecologically significant components of Mediterranean vegetation. The *Medicago rigidula* complex, comprising *M. rigidula*, *M. rigiduloides*, *M. sinskiae*, and *M. constricta*, has undergone substantial taxonomic revision recently, but species boundaries remain unclear due to overlapping morphological traits, recent divergence, and selfing reproductive strategies. To clarify species relationships within the complex, we conducted an integrative analysis of populations sampled from diverse regions of Iran. Floral morphology (34 characters), anatomical features (17 characters), palynology, and seed micromorphology were studied using light and SEM microscopy. Morphological and anatomical differences, particularly in floral characters, pollen aperture types, seed surface vesiculation, and pod vascular bundle shape, helped discriminate among taxa. Phylogenetic analyses based on combined ITS and ETS nuclear ribosomal DNA sequences supported the distinctiveness of *M. constricta* and *M. sinskiae*, while also validating the separation of *M. rigidula* and *M. rigiduloides* despite partial morphological overlap. A new ETS primer pair, designed specifically for the core *Medicago* group, improved amplification success and resolution. Cluster and PCA analyses of floral characters further supported species-level distinctions. Although clinal variation was observed in pod morphology, integration of multiple data sources enabled more robust species delimitation. Our findings underscore the importance of combining multilocus molecular data with detailed morphological and anatomical traits to resolve taxonomic complexity in recently diverged, selfing taxa. An updated identification key for the *M. rigidula* complex is provided, contributing to the systematics within the group.

Keywords: Annual medics; Iran; Mediterranean region; primer design; speciation; taxonomy

فیلوژنی و تعیین حدود گونه ها در کمپلکس گونه ای ***Medicago rigidula* (L.) All.** بر اساس داده‌های توالی **nrDNA**

زهرا قربانی: مربی گروه علوم گیاهی، دانشکده علوم زیستی، دانشگاه خوارزمی، تهران

ایرج مهرگان: دانشیار گروه زیست شناسی، دانشگاه آزاد واحد علوم تحقیقات، تهران

مصطفی اسدی: استاد پژوهش، موسسه تحقیقات جنگلها و مراتع کشور، سازمان تحقیقات، آموزش و ترویج کشاورزی، تهران

ارنست اسمال: موسسه تحقیقاتی بیوسیستماتیک، وزارت کشاورزی کانادا، اوتاوا، اونتاریو، کانادا

چکیده: گونه‌های یک‌ساله جنس *Medicago* (تیره باقلائیان) از اجزای مهم پوشش گیاهی در ناحیه مدیترانه‌ای به شمار می‌روند. مجموعه‌ی *Medicago rigidula* که شامل گونه‌های *M. rigidula*، *M. rigiduloides*، *M. sinskiae* و *M. constricta* می‌باشد، در سال‌های اخیر دستخوش بازنگری‌های تاکسونومیکی قابل توجهی شده است. با این حال، به دلیل شباهت‌های ریخت‌شناسی، واگرایی افراد و سامانه تولیدمثل خودگشن، مرزهای گونه‌ای در این مجموعه همچنان مبهم باقی مانده‌اند. به‌منظور روشن‌سازی روابط گونه‌ای، جمعیت‌هایی از مناطق مختلف ایران مورد بررسی قرار گرفتند. ریخت‌شناسی گل (۳۴ صفت)، ویژگی‌های تشریحی (۱۷ صفت)، ساختار دانه گرده و میکرومورفولوژی بذر با استفاده از میکروسکوپ نوری و الکترونی روبشی (SEM) مطالعه شد. تفاوت‌های ریختی و تشریحی به‌ویژه در صفات گل، نوع منفذ دانه‌های گرده، ساختار سطح بذر و شکل دسته‌های آوندی در نیام، موجب تمایز بین گونه‌ها گردید. تجزیه‌های فیلوژنتیکی مبتنی بر توالی‌های ترکیبی ITS و ETS، موقعیت مجزای گونه‌های *M. constricta* و *M. sinskiae* را تأیید کردند و همچنین جدایی *M. rigidula* و *M. rigiduloides* را با وجود هم‌پوشانی‌های جزئی در ریخت‌شناسی تأیید نمودند. آغازگر جدیدی برای ناحیه ETS طراحی شد که موجب بهبود موفقیت در تکثیر و افزایش وضوح نتایج گردید. تحلیل‌های خوشه‌ای و PCA نیز از تفکیک گونه‌ای حمایت کردند. با وجود مشاهده تغییرات تدریجی در ریخت‌شناسی نیام، تلفیق داده‌های مولکولی و ریختی امکان تعیین دقیق‌تر حدود گونه‌ها را فراهم ساخت. کلید شناسایی بروز شده برای مجموعه *M. rigidula* نیز ارائه شده است.

INTRODUCTION

The genus *Medicago* L. (Fabaceae; tribe Trifolieae; subtribe Trigonellinae), in its modern circumscription, includes over 80 species of annual, biennial, and perennial herbs, along with a few shrubs, native to Eurasia (Small & Jomphe 1989; Small 2011). The subtribe Trigonellinae includes three genera (*Medicago*, *Trigonella* L., and *Melilotus* L.), all characterized by trifoliolate leaves and stipules that are adnate to the stem but do not completely encircle it (Small 1987). The generic boundaries between *Medicago* and *Trigonella* have been revised over time (Small & al. 1987; Small & Jomphe 1989; Small 2011; Steele & al. 2010). In its current definition, *Medicago* includes the "medicagoid" species formerly placed in sections *Buceras* and *Lunatae* of the genus *Trigonella* (Small 2011). All species of *Medicago* exhibit an explosive pollination syndrome (Small & al. 1987). The monophyly of *Medicago*, initially proposed by Small & al. (1987), has been supported by analyses using various molecular markers (Bena & al. 1998a; Bena 2001; Steele & Wojciechowski 2003; Wojciechowski & al. 2004; Downie & al. 1998; Maureira-Butler & al. 2008; Steele & al. 2010).

The perennial species of *Medicago* include the economically important *M. sativa* L. (alfalfa), and the classification of most of these has been studied intensively. However, the taxonomy of a large group of annual species of *Medicago* with coiled fruits (*Medicago* section *Spirocarpos* Ser.) has been disputed even recently (Small 2011). Some of these species differ in subtle or minor characteristics, which seem to be maintained by inbreeding, and several new species have only been discovered recently (Small 1990, 2011).

The generic name *Medicago* was first effectively erected by Linnaeus (1753), who included eight species. Most of the original annual Linnaean species of *Medicago* were first regarded as 13 varieties of *M. polymorpha* L. (Linnaeus 1753). Those varieties were elevated to species by more recent botanists such as Miller (1768) and Allioni (1785). The very polymorphic species *M. rigidula* (L.) All. (Allioni 1785) was introduced as *M. polymorpha κ rigidula* by Linnaeus (1753). Pods of this species are very variable in form, size, appression of coils, form and size of spines, edge of coils, and indumentum (Mehregan & al. 2002). Taxonomy of the species has long been considered to be problematic (see Heyn 1963 and 1970 for details). Heyn (1963, 1984) distinguished three varieties *rigidula*, *submitis* (Boiss.) Heyn, and *agrestis* Burn. under *M. rigidula*. However, Small & Jomphe (1989) accepted no infraspecific division of the species. Small & al. (1990) found morphological differences between the European and the Asian populations of the species. Small (1990) segregated the Asian populations

under the new name *M. rigiduloides* E. Small. Mehregan & al. (2002) suggested that populations of *M. rigidula* should not be divided into distinct groups due to the presence of a clinal variation in their morphological characters. Instead, they introduced a wider concept for *M. rigidula*, including two other close species, *M. constricta* Durieu and *M. sinskiae* Uljanova. *Medicago rigidula* was divided into three subspecies i.e., subsp. *rigidula*, subsp. *sinskiae* (Uljanova) Mehregan & Rahimin. and subsp. *constricta* (Durieu) Ponert by Mehregan & al. (2002). In Flora of Iran (Mehregan & Small 2023), *M. rigidula* and *M. rigiduloides* are recognized as separate species, but the specimens with intermediate characters are cited under the name *M. rigidula* s.l.

The complexity of *Medicago rigidula* and its allied species has been demonstrated by several authors (Heyn 1963, 1984; Small & al. 1990; Mehregan & al. 2002). Various molecular studies have confirmed their close phylogenetic relationships, and they are collectively referred to here as the *Medicago rigidula* complex (Bayat & al. 2021a, 2021b). According to Downie & al. (1998), maximum parsimony analysis of the internal transcribed spacer (ITS) dataset produced a poorly supported monophyletic clade (bootstrap support [BS] = 40%) comprising *M. rigidula*, *M. rigiduloides*, *M. sinskiae*, and *M. constricta*, which formed within a larger polytomy. Using ITS and external transcribed spacer (ETS) markers, Bena & al. (1998a, 1998b) found a close relationship between *M. rigidula* and *M. constricta*. In a subsequent study, Bena & al. (1998c) identified a well-supported clade (BS = 83%) consisting of *M. rigidula*, *M. rigiduloides*, and *M. constricta*, with *M. noeana* as the sister taxon, based on a strict consensus tree from maximum parsimony analysis of combined ITS and ETS data.

In contrast to the unresolved relationship between *M. rigidula* and *M. constricta* revealed by Bayesian analysis of the nuclear gene *β-cop*, these species appeared monophyletic in a similar analysis of the nuclear gene *CNGC5* (Maureira-Butler & al. 2008). Using chloroplast (*trnK/matK*) and nuclear (*GA3ox1*) markers, Steele & al. (2010) found no evidence of close phylogenetic relationships between *M. rigidula* and *M. constricta*. Among previous studies, only that of Downie & al. (1998) included all members of the complex; however, their analysis was based solely on the ITS region. More recently, structure analysis of microsatellite (SSR) data by Bayat & al. (2021b) revealed two genetically distinct groups with significant internal homogeneity, likely shaped by a predominantly selfing mating system. These groups were consistently supported by multiple clustering methods, providing strong molecular evidence for the separation of *M. rigidula* and *M. rigiduloides*.

Iran and parts of the surrounding region are unique in that they represent all members of the *Medicago rigidula* complex (Mehregan & al. 2002; Bayat & al. 2021a, 2021b; Zareei et al. 2022). This provides a valuable opportunity to examine in detail the taxonomic segregation and phylogenetic relationships of the four putative species within the complex. The main aims of this study are to assess the separability and interrelationships of *M. rigidula*, *M. rigiduloides*, *M. sinskiae*, and *M. constricta* using an integrative approach. To achieve this, we employed (1) phylogenetic analysis based on nuclear ribosomal ITS and ETS markers, (2) comparative analysis of anatomical and morphological characters, including stem and pod anatomy as well as floral and fruit morphology, and (3) expanded sampling across the full geographic range of the complex within Iran. This comprehensive approach is intended to clarify species boundaries, test previous taxonomic hypotheses, and contribute to a more robust understanding of the evolutionary history of the *M. rigidula* complex.

MATERIALS AND METHODS

Sampling and molecular analyses

More than 130 herbarium specimens representing different members of the *Medicago rigidula* complex were examined morphologically (listed in Mehregan & Small 2023). These included *M. rigidula* (50 accessions), *M. rigiduloides* (17 accessions), *M. sinskiae* (3 accessions), and *M. constricta* (13 accessions), all collected from various regions of Iran. Total genomic DNA was extracted either from silica-gel-dried leaves of field-collected specimens or from herbarium material deposited in IAUH (Islamic Azad University Herbarium) and TARI (Herbarium of the Research Institute of Forests and Rangelands) (Table 1). DNA extraction followed a modified CTAB protocol (Doyle and Doyle 1987) using NucleoSpin® Plant Kits (Macherey-Nagel, Düren, Germany), following the manufacturer's instructions.

nrDNA ITS

The complete internal transcribed spacer (ITS) region (ITS1 + 5.8S + ITS2) was amplified using the primers AB101 (5′-ACG AAT TCA TGG TCC GGT GAA GTG TTC G-3′) and AB102 (5′-TAG AAT TCC CCG GTT CGC TCG CCG TTA C-3′), as described by Douzery & al. (1999). PCR amplification was performed under the following conditions: initial denaturation at 95°C for 5 minutes; 35 cycles of 30 seconds at 95°C, 30 seconds at 50°C, and 1 minute 30 seconds at 72°C; followed by a final extension at 72°C for 7 minutes. PCR products were purified using the NucleoSpin® Extract Kit (Macherey-Nagel) according to the manufacturer's protocol.

Table 1. List of taxa, localities, and GenBank accession number of material used in the molecular phylogenetic analysis. Asterisks (*) indicate the material used in the SEM microscopy.

No	**Taxa**	**Collection data**	**Genbank code**	
			ITS	ETS
1	*Medicago constricta* Durieu	Iran: Kohgilouyeh and Boyer-Ahmad, Boustan, 48 km from Gachsaran to Shiraz, 2 km SE of Boustan, Mehregan & Yeganeh 000014385 (IAUH)*	KX027586	KX027569
2	*M. constricta* Durieu	Iran: Lorestan, Sepiddasht, Ghorbani 000014386 (IAUH)	KX027585	KX027572
3	*M. constricta* Durieu	Iran: Khoozestan, Masjedsoleyman, Lali, Tugah Foroughi 3207 (TARI)	KX027592	KX027580
4	*M. rigidula* (L.) All.	Iran: Mazandaran, Chalous, ca. 5 km from Marzan-Abad towards Karaj, Mehregan & Yeganeh 000014384 (IAUH)*	KX027589	KX027576
5	*M. rigidula* (L.) All.	Iran: Gorgan, 22 km to Maravetappeh on the road, from Inche_ Boroon (CG3), Assad i& Massoumi 55432 (TARI)	KX027582	KX027579
6	*M. rigiduloides* E. Small	Iran: Lorestan, Sepiddasht, Ghorbani 000014387 (IAUH)*	KX027584	KX027570
7	*M. rigiduloides* E. Small	Iran: Khorassan, Darre-Gaz, Park-e Tandure, Mozaffarian 67734 (TARI)	KX027591	KX027578
8	*M. rigiduloides* E. Small	Iran: Tehran, Boumehen on Abaliroud, Dini & Azarm 11815 (TARI)	KX027590	KX027575
9	*M. rigiduloides* E. Small	Iran: Hormozgan, Bandar-Abbas, Haji-Abad, Mozaffarian 52130 (TARI)	KX027583	KX027571
10	*M. rigiduloides* E. Small	Iran: Lorestan, Khorram-Abad, 35 km Khorram-Abad to Andimeshk, Ghorbani 000014388 (IAUH)*	-	-
11	*M. rigiduloides* E. Small	Iran: Kermanshah, Ravansar, 2 km from Ravansar to Paveh, Ghorbani 000014389 (IAUH)*	-	-
12	*M. sinskiae* Uljan.	Iran: Lorestan, Khorram-Abad, 35 km Khorram-Abad to Poldokhtar, Ghorbani 000014381 (IAUH)	KX027587	KX027577
13	*M. sinskiae* Uljan.	Iran: Lorestan, Sepiddasht, Ghorbani 000014383 (IAUH)*	KX027588	KX027574
14	*M. sinskiae* Uljan.	Iran: Lorestan, Khoram-Abad, 30 km Khorram-Abad to Poldokhtar, Ghorbani 000014382 (IAUH)*	KX027581	KX027573

nrDNA ETS

Bena & al. (1998a) were unable to identify *Medicago*-specific primers for ETS and therefore amplified the entire intergenic spacer (IGS) using universal primers (18S-IGS and 26S-IGS) originally developed by Baldwin and Markos (1998). As no ETS-specific primers existed for *Medicago*, we designed a new primer pair based on previously published *Medicago* ETS sequences (Bena & al. 1998a). The newly designed forward primer MEDIC-F (5′-GKG TGG GAT GTT CYG YGA T-3′) and reverse primer MEDIC-R (5′-GAC TAC TGG CAG GAT CAA CCA-3′) amplify approximately 460 bp of the ETS region and appear to be genus-specific. PCR amplification conditions were as follows: initial denaturation at 95 °C for 5 minutes; 35 cycles of 30 seconds at 95 °C, 30 seconds at 59 °C, and 1 minute 30 seconds at 72 °C; followed by a final extension at 72 °C for 8 minutes.

The resulting ITS and ETS sequences were manually edited and assembled using Sequencher 4.1.2 (Gene Codes Corporation, Ann Arbor, Michigan, USA). Our newly generated sequences, together with additional sequences obtained from GenBank (Appendix 1), were aligned using MacClade 4.08 (Maddison and Maddison 2005). As GenBank accessions lacked 5.8 region, we removed that part from the whole data matrix.

Phylogenetic analyses

Parsimony analysis (MP): Parsimony analyses of the ITS, ETS, and combined ITS+ETS datasets were conducted using *PAUP 4.0b8** (Swofford 2002). To identify the most parsimonious trees, heuristic searches were performed under the following settings: stepwise taxon addition, tree bisection-reconnection (TBR) branch swapping, and 100 replicates. For each dataset, all obtained shortest trees were summarized into a strict consensus tree. Tree length (TL), consistency index (CI), and retention index (RI), excluding uninformative characters, were calculated for each strict consensus tree (Table 2). Bootstrap support values (Felsenstein 1985) were estimated for each node using 100 replicates of a heuristic search, with random taxon addition (10 replicates per bootstrap replicate) and no branch swapping.

Table 2. Numerical results of the analyses of the aligned ITS, ETS, and combined ITS + ETS datasets.

Characters	ITS	ETS	Combined ITS + ETS
Total characters	481	453	934
Constant characters	307	232	539
Parsimony uninformative	63	82	145
Parsimony informative	111 (23 %)	139 (30 %)	250 (26.7 %)
Tree length (consensus tree)	301	446	753
CI (consensus tree)	0.694	0.668	0.673
RI (consensus tree)	0.820	0.759	0.781

Bayesian inference (BI): Bayesian analyses of the ITS, ETS, and combined datasets were performed using MrBayes v3.1.2 (Ronquist & al. 2005). Before analysis, the best-fit models of nucleotide substitutions were selected using Modeltest v3.7 (Posada and Crandall 1998) under the Akaike Information Criterion (AIC), based on likelihood scores computed via likelihood ratio tests (Felsenstein 1988) implemented in PAUP*. Bayesian inference was conducted with four Markov chains (three heated, one cold) running simultaneously for 5,000,000 generations. Trees were sampled every 100 generations, and the first 25% of trees were discarded as burn-in. The remaining 37,500 post-burn-in trees were used to generate a 50% majority-rule consensus tree with posterior probability values.

Morphological analyses

The most important diagnostic differences among species of the *Medicago rigidula* complex are found in reproductive structures. In this study, the morphology of opened flowers and mature pods was carefully examined. A representative subset of specimens was randomly selected and analyzed (Table 1). For floral morphology, a total of 34 qualitative and quantitative characters were measured and recorded (Table 3). In anatomical analyses, 17 characters were similarly assessed (Table 4). Cluster analysis of the morphological data was performed using the method described by Small & al. (1990).

Pollen grains were extracted from unopened flowers and subjected to acetolysis following the standard protocol of Erdtman (1960). Pollen morphology was examined using both light microscopy and scanning electron microscopy (SEM). For SEM imaging, pollen grains were coated with a thin layer of gold using a BAL-TEC SCD005 sputter coater (BAL-TEC, Switzerland) and observed with an XL30 Scanning Electron Microscope (Philips, the Netherlands).

Ripe seeds were extracted from mature pods, gold-coated, and photographed using the same SEM preparation and equipment as for pollen. For anatomical studies, young stems, the midribs of middle leaflets, and immature pods were cross-sectioned, stained, and prepared for light microscopy according to the protocol of Azizian and Cutler (1982).

RESULTS

Molecular analyses

The numerical results of the phylogenetic analyses of the ITS, ETS, and combined ITS+ETS datasets were summarized in Table 2. The evolutionary models and corresponding maximum likelihood parameters used in MrBayes were as follows: ITS dataset: Model selected: TrN+G, Gamma distribution shape parameter (G) = 0.5985. ETS dataset: Model selected: TVM+G, Gamma distribution shape parameter (G) = 0.8197. Combined ITS + ETS dataset: Model selected: GTR+G, Gamma distribution shape parameter (G) = 0.5956.

MP analyses of three datasets (ITS, ETS, and ITS+ETS) did not result in a single most parsimonious tree for each dataset. Therefore, the 10,000 shortest trees from each analysis were summarized into a strict consensus tree. The ITS and ETS datasets were congruent and yielded broadly similar phylogenetic patterns (not shown). Since the Maximum parsimony (MP) analysis of the combined ITS+ETS dataset produced a tree topology largely consistent with its Bayesian tree, only the 50% majority-rule consensus tree derived from the Bayesian analysis of the combined dataset is presented here (Fig. 1).

As shown in Fig. 1, all *Medicago* species included in the analyses formed a strongly supported monophyletic clade (BS = 100% in all datasets). While major clades within *Medicago* were retrieved, relationships among them remained largely unresolved at deeper (distal) nodes. The species of the *M. rigidula* complex—*M. rigidula*, *M. rigiduloides*, *M. sinskiae*, and *M. constricta*—along with *M. noeana* Boiss., formed a well-supported monophyletic group in both ETS and combined ITS + ETS analyses (BS = 57% and PP = 0.96 for ETS; BS = 76% and PP = 0.98 for the combined dataset).

Table 3. Selected quantitative and qualitative characters from the floral morphology of taxa belonging to the *Medicago rigidula* complex. The measures represent means ± standard deviation. Characters: 1= Calyx tube length; 2= Calyx tube width; 3= Ratio of calyx tube length to its width; 4= Calyx lobe length; 5= Ratio of calyx lobe to calyx tube length; 6= Standard length; 7= Standard width; 8= Claw of standard length; 9= Wing limb length; 10= Wing limb width; 11= Ratio of length to width wing limb; 12= Claw of wing; 13= Horn of wing length; 14= Horn of wing width; 15= Ratio of length to width horn of wing; 16= Keel limb length; 17= Keel limb width; 18= Ratio of length to width of keel limb; 19= Keel claw; 20= Lamb of limb of keel length; 21= Lamb of limb of keel width; 22= Ratio of length to width Lamb of limb of keel; 23= Fused filament column length; 24= Filament; 25= Ratio of Fused filament column to filament; 26= Ovary length; 27= Style; 28 = Claw of ovary length; 29= Ratio of ovary to style; 30= Ratio of ovary to calw; 31= Calyx color; 32= Standard form; 33= Standard apex; 34 = Ratio of corolla to calyx (terminology after Small, 2011).

	Quantitative characters										
Taxa	**1**	**2**	**3**	**4**	**5**	**6**	**7**	**8**	**9**	**10**	**11**
Medicago rigidula	1.45± 0.12	1.76 ±0.14	0.83 ±0.13	1.10 ±0.12	0.76 ±0.21	2.56 ±0.16	2.31 ±0.95	0.38 ±0.16	1.50 ±0.62	0.64 ±0.96	2.36 ±0.24
M. rigiduloides	1.38± 0.28	1.97 ±0.34	0.71 ±0.15	1.62 ±0.39	1.16 ±0.16	3.37 ±0.54	2.83 ±0.78	0.38 ±0.21	2.07 ±1.00	1.03 ±0.48	2.03 ±0.26
M. sinskiae	1.73± 0.45	2.36 ±0.39	0.75 ±0.25	2.17 ±0.43	1.28 ±0.21	3.90 ±0.38	3.29 ±0.27	0.55 ±0.99	1.61 ±0.27	1.19 ±0.29	1.39 ±0.24
M. constricta	1.41± 0.98	2.37 ±0.25	0.60 ±0.32	0.95 ±0.33	0.67 ±0.21	2.63 ±0.40	2.36 ±0.26	0.23 ±0.40	1.41± 0.26	0.73 ±0.23	2.00 ±0.33

	Quantitative characters										
Taxa	**12**	**13**	**14**	**15**	**16**	**17**	**18**	**19**	**20**	**21**	**22**
M. rigidula	0.91± 0.22	0.47± 0.60	0.31± 0.40	1.53± 0.36	1.33± 0.85	0.74± 0.49	1.79± 0.18	1.16± 017	0.25± 0.006	0.28± 0.35	0.88± 0.91
M. rigiduloides	1.74± 0.73	0.32± 0.14	0.39± 0.15	1.15± 1.03	1.70± 0.44	0.99± 0.28	1.73± 0.17	1.80± 0.41	0.25± 0.26	0.59± 0.81	0.42± 0.49
M. sinskiae	1.28± 0.27	0.46± 0.63	0.33± 0.48	1.38± 0.17	1.79± 0.12	1.18± 0.10	1.50± 0.13	1.86± 0.19	0.23± 0.53	0.47± 0.13	0.49± 0.73
M. constricta	0.96± 0.80	0.24± 0.46	0.32± 0.46	0.74± 0.66	1.49± 0.16	0.85± 0.12	1.75± 0.17	1.69± 0.11	0.32± 0.99	0.45± 0.77	0.70± 0.13

	Quantitative characters							**Qualitative**				
Taxa	**23**	**24**	**25**	**26**	**27**	**28**	**29**	**30**	**31**	**32**	**33**	**34**
M. rigidula	2.42± 0.12	0.40± 0.21	0.16± 0.10	1.54± 0.47	0.87± 0.19	0.25± 0.61	0.60± 0.23	0.19± 0.25	Green	Ovate	Dented	1:1
M. rigiduloides	2.60± 0.69	0.56± 0.16	0.21± 0.16	1.44± 0.31	1.37± 0.52	0.46± 0.14	0.93± 0.22	0.31± 0.37	Green	Ovate	Circular-dented	1:1, 1:2
M. sinskiae	2.55± 0.17	0.50± 0.47	0.20± 0.20	1.21± 0.51	1.28± 0.65	0.50± 0.22	1.31± 0.75	0.41± 0.47	Green	Elliptic-ovate	Dented	1:1
M. constricta	2.84± 0.12	0.73± 0.14	0.25± 0.36	1.59± 0.48	1.08± 0.12	0.21± 0.10	0.71± 0.21	0.14± 0.32	Green-purple	Ovate	Circular	3:1

In both analyses, *M. noeana* was found to be the sister taxon to the rest of the *M. rigidula* complex. All members of the *M. rigidula* complex were recovered as monophyletic in both MP and Bayesian analyses of the ETS and combined datasets (BS = 56% and PP = 0.82 for ETS; BS = 75% and PP = 0.97 for combined). Although this monophyly was not recovered in the MP analysis of the ITS dataset, it was weakly supported in the Bayesian analysis (PP = 0.81). *Medicago constricta* was resolved as sister to the remaining species of the *M. rigidula* complex in both ETS and combined datasets (Fig. 1). All samples of *M. constricta* formed a highly supported monophyletic clade in both MP and Bayesian analyses across all datasets (BS = 100%, PP = 1.0). The remaining members of the complex—*M. sinskiae*, *M. rigidula*, and *M. rigiduloides*—also

formed a monophyletic group in all analyses (BS = 94% and PP = 1.0 for ITS; BS = 65% and PP = 0.88 for ETS; BS = 98% and PP = 1.0 for the combined dataset), with *M. sinskiae* resolved as sister to *M. rigidula* and *M. rigiduloides*.

The ITS dataset alone was insufficient to differentiate *M. rigidula* from *M. rigiduloides*. However, two accessions of *M. rigidula* formed a monophyletic clade in both MP and Bayesian analyses of the ETS and combined datasets (BS = 75%, PP = 0.99 for ETS; BS = 79%, PP = 0.99 for combined). Similarly, five accessions of *M. rigiduloides* formed a monophyletic clade in ETS and combined dataset analyses (BS = 61% and PP = 0.98 for ETS; BS = 59% and PP = 0.98 for combined).

Morphological analysis

Our results showed clear differences in qualitative and quantitative floral morphology characters among the studied taxa (Table 3). Cluster analysis of floral morphological data revealed that while some partial clusters corresponded to individual species, others contained mixed accessions, suggesting intermediate morphotypes (Fig. 2). Principal Component Analysis (PCA) further supported this finding: *M. constricta* samples formed a distinct cluster, clearly separated from those of *M. rigidula*, *M. rigiduloides*, and *M. sinskiae*, which together formed an intermixed group (Fig. 3).

Quantitative traits particularly diagnostic for *M. sinskiae* included larger standard petal size (standard length: 3.90 ± 0.38 mm, width: 3.29 ± 0.27 mm) and calyx measurements (tube length: 1.73 ± 0.45 mm; lobe length: 2.17 ± 0.43 mm) compared to the other taxa. *M. rigiduloides* also showed larger standards (length: 3.37 ± 0.54 mm) and wings (limb length: 2.07 ± 1.00 mm) than *M. rigidula* and *M. constricta*. Conversely, *M. constricta* exhibited the smallest wing claws (0.23 ± 0.40 mm) and short calyx lobes (0.95 ± 0.33 mm), reinforcing its morphological divergence.

In terms of qualitative floral traits, *M. constricta* was unique in having a green-purple calyx, ovate standards with circular apices, and a 3:1 corolla-to-calyx ratio—the latter significantly different from the consistent 1:1 ratio seen in *M. rigidula* and *M. sinskiae*. These features support *M. constricta*'s taxonomic separation within the complex.

Table 4. Selected quantitative and qualitative characters from the anatomy of taxa belonging to *M. rigidula* complex. The measures represent min-max in micrometers. Characters: 1= Length of vascular bundles cross-section in stem; 2= Width of vascular bundles cross-section in stem; 3= Ratio of character 2 to character 3; 4= Number of vascular bundles in stem cross section; 5= Number of collenchymatous tissue layers in stem cross-section; 6= Average of length of vascular bundle cross-section in stems; 7= Average of width of vascular bundles cross-section in stems; 8= Length of vascular bundle cross-section in leaflet; 9= Width of vascular bundles cross-section in leaflet; 10= Ratio of length to width of vascular bundle cross-section in leaflet; 11= Thickness of dermis from epidermis to vascular bundles in leaflet; 12= Outline of middle vascular bundle in leaflet; 13= Midrib outline; 14= Shape of coil edge in pods; 15= Shape of vascular bundles in edge of coils; 16= Number of base cells in glandular hairs in pod; 17= Number of coils in pod.

Taxa	**1**	**2**	**3**	**4**	**5**	**6**	**7**	**8**	**9**	**10**	**11**	**12**	**13**	**14**	**15**	**16**	**17**
M. rigidula	0.26-0.63	0.17-0.58	1.27-1.33	10-12	4-5	0.36-0.46	0.27-0.36	0.24-0.36	0.27-038	0.88-0.94	0.17-0.27	Ovate-Broad ovate	U-form	Rounded	Rounded	1-3	4
M. rigiduloides	0.12-0.63	0.11-0.50	1.20-1.44	11-14	4-6	0.34-0.42	0.27-0.30	0.32-0.41	0.25-0.33	1.18-1.32	0.15-0.37	Spherical-Ovate	U-form	Rounded	Rounded	2-4	4-6
M. sinskiae	0.20-0.67	0.14-0.65	1.22-1.38	10-12	6-8	0.35-0.47	0.27-0.35	0.15-0.25	0.13-0.23	1.08-1.15	0.11-0.15	Spherical	Flat, U-form	Rounded	Ovate	1-2	2-3
M. constricta	0.12-0.45	0.10-0.47	1.10-1.28	12	5	0.27-0.33	0.21-0.30	0.29-0.32	0.22-0.25	1.16-1.45	0.06-0.10	Ovate	Flat, U-form	Truncated	Cuneate	1-4	5-6

Pollen and seed micromorphology

Pollen grains of all taxa were isopolar and zonocolporate (Fig. 4), but differed in aperture types. *Medicago constricta*, *M. sinskiae*, and *M. rigidula* had predominantly tri-zonocolporate pollen, while *M. rigidula* also exhibited tetra-zonocolporate grains, occasionally within a single flower, indicating notable intra-individual variability.

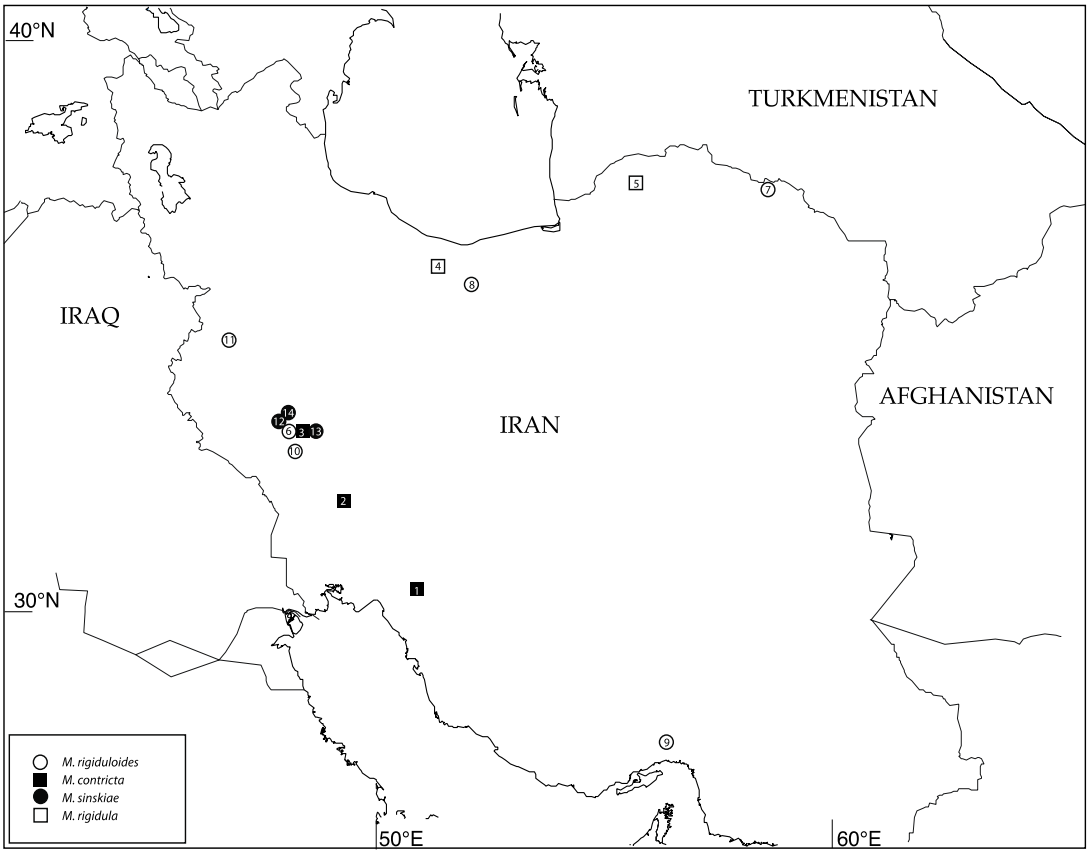

Fig. 1. Map showing the localities of collected material examined in the molecular study. Details of the samples are given in Table 1.

All species shared a prolate-spheroidal shape and mesocolpial ornamentation composed of anastomosing striae. The co-occurrence of tri- and tetra-zonocolporate pollen in *M. rigidula* aligns with its broader floral character variability observed in PCA and cluster analyses.

Seed coat micromorphology under SEM revealed diagnostic differences in surface ornamentation (Fig. 5). *Medicago sinskiae* and *M. constricta* displayed elevated vesicles completely covering the edges of the reticulum, while *M. rigidula* and *M. rigiduloides* had non-elevated or partially elevated vesicles, exposing the reticulum margins. These structural differences in seed coat vesiculation likely correspond to species-specific ecological strategies or developmental processes, reinforcing taxonomic boundaries within the complex.

Anatomical characters

Previous studies indicated that pods (Fig. 6) are highly variable in form and size, and exhibit clinal variation in morphological characters (Small & al. 1990; Mehregan & al. 2002). Our own analysis of external pod morphology yielded admixed results (not shown), reflecting continuous variation and overlapping features among species. However, anatomical studies revealed more reliable differences between specimens (Table 4; Fig. 6).

Young stems across all taxa were irregularly 4-angled, but differed in the number of collenchymatous layers at the angles and the number of vascular bundles. For example, *M. rigiduloides* had up to 14 vascular bundles and 4–6 collenchymatous layers, whereas *M. sinskiae* showed 6–8 collenchymatous layers**,** the highest among the studied taxa. These variations indicate species-specific stem structural adaptations.

Leaflets were generally flat to keeled, with flat to elevated veins on the abaxial surface. Midrib outlines varied: in *M. sinskiae* and *M. constricta* exhibited flat to U-form midribs, whereas *M. rigidula* and *M. rigiduloides* primarily had U-shaped midrib outlines. Dermal tissue thickness from epidermis to vascular bundle was greatest in *M. sinskiae* (up to 0.15 mm) and thinnest in *M. constricta* **(**0.06–0.10 mm**),** providing another layer of anatomical distinction.

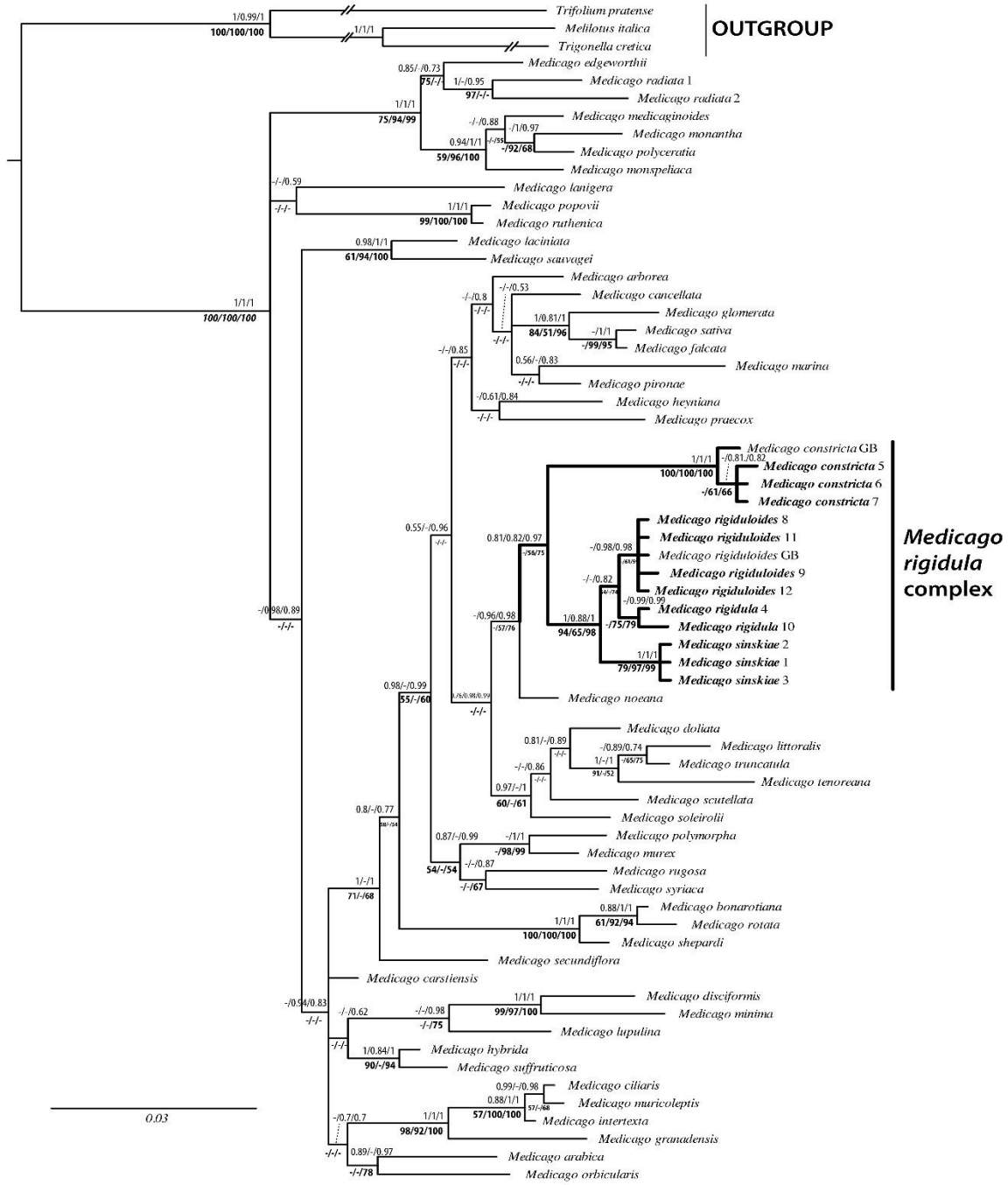

Fig. 2. Phylogeny of *Medicago* species based on Bayesian analyses of the combined ITS + ETS datasets. Numbers above branches are posterior probabilities; numbers below branches are bootstrap values for those branches retrieved in maximum parsimony analyses of the ITS, ETS, and combined ITS + ETS datasets (from left to right: ITS / ETS / combined ITS + ETS).

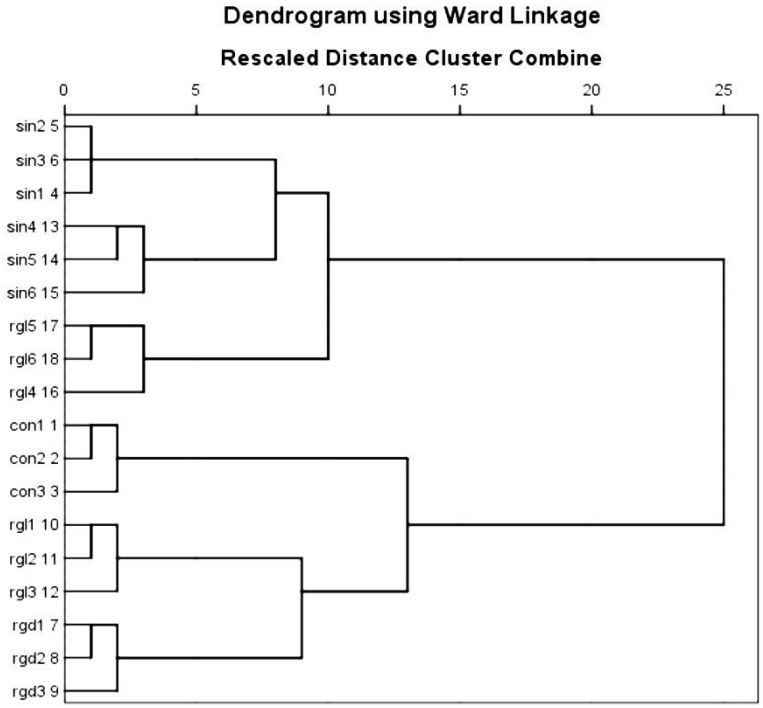

Fig. 3. Dendrogram illustrating the clustering of 18 populations (Table 1) of the *M. rigidula* complex based on analysis of 34 floral characters listed in Table 3. Abbreviations: sin (*M. sinskiae*), rgl (*M. rigidula*), rgd (*M. rigiduloides*), con (*M. constricta*).

Cross-sectional analysis of young pods also showed meaningful interspecific differences. Notably, *Medicago constricta* had coils with truncated edges and cuneate vascular bundles, a trait absent in other species. In contrast, *M. sinskiae*, *M. rigidula*, and *M. rigiduloides* had rounded pod coils with ovate to rounded vascular bundles at the edges (Fig. 6). Additionally, the number of coils per pod was highest in *M. constricta* (5–6 coils) and lowest in *M. sinskiae* (2–3 coils), while the number of basal cells in glandular hairs ranged from 1–2 in *M. sinskiae* to up to 4 in *M. constricta*. These anatomical traits together support the distinctiveness of *M. constricta* within the *M. rigidula* complex.

DISCUSSION

Our results show that the relationships inferred from phylogenetic analysis showed a notable level of congruence with morphological, anatomical, and palynological data across the *Medicago rigidula* complex. *M. constricta* was clearly distinguished both genetically, forming a distinct clade, and morphologically, with unique floral traits and seed surface ornamentation. Palynological features and the elevation of seed coat vesicles further supported its separation. *M. sinskiae* also showed consistent differentiation in seed and pollen morphology, anatomy of pod vasculature, and a distinct phylogenetic position. While *M. rigidula* and *M. rigiduloides* exhibited overlapping morphological and anatomical traits, such as similar flower dimensions and stem anatomy, they were also separated in the molecular analyses, suggesting cryptic divergence not fully captured by phenotype alone. Thus, the integration of floral morphology, seed and pollen micromorphology, and internal anatomical structures with nuclear phylogenetic markers (ITS and ETS) provided a robust framework for resolving species boundaries within this complex group.

Species delimitation in closely related plant taxa is often challenging due to rapid and recent phylogenetic divergence, high phenotypic plasticity, introgression, and partial barriers to gene flow (Shaffer & Thomson 2007). This is particularly true for self-mating annual species such as those in the genus *Medicago*, where single-marker approaches frequently fail to provide sufficient resolution. Selfing species typically exhibit low genetic variation within populations and high genetic similarity between populations, primarily due to limited gene flow and strong genetic drift (Bena 2001; Ronfort & al. 2006).

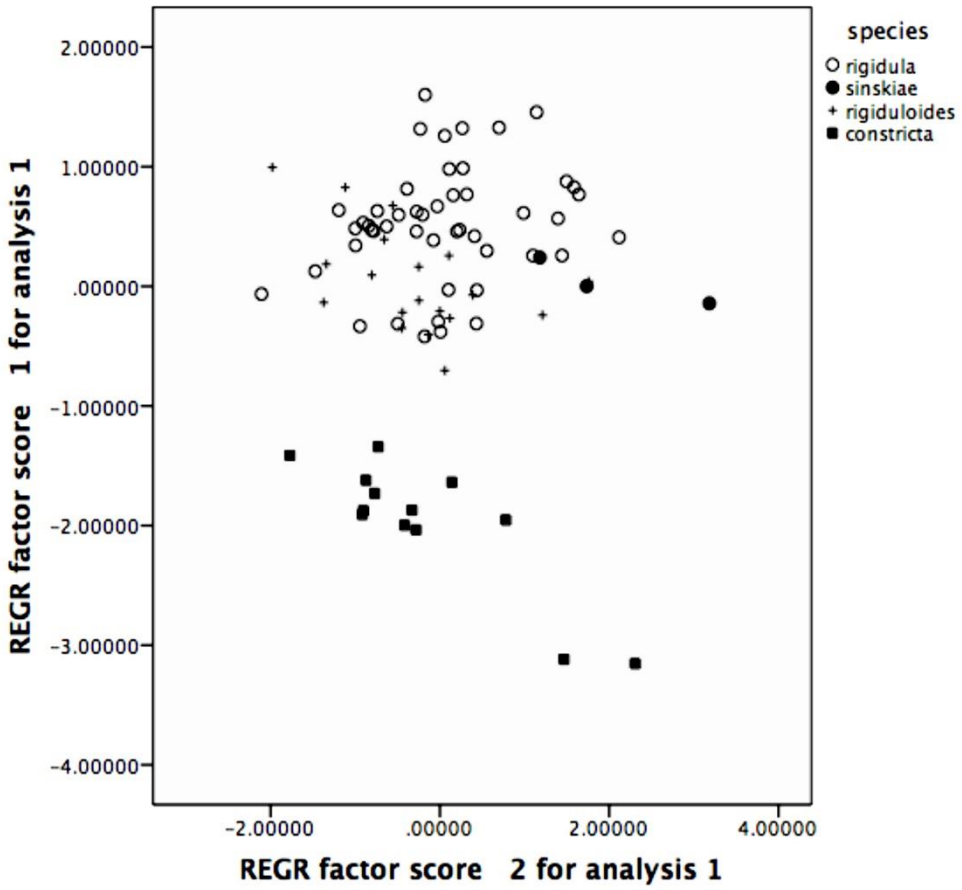

Fig. 4. Two-dimensional PCA plot based on morphological characters of different species of the *M. rigidula* complex.

In *Medicago*, traditional molecular markers such as ITS regions, plastid sequences, or microsatellites often lack the discriminatory power to distinguish recently diverged taxa because they cannot fully capture subtle genomic differences driven by reproductive isolation and local adaptation (Branca & al. 2011). Moreover, the rapid life cycle and reproductive assurance of selfing can cause repeated founder effects that reduce effective population size and further homogenize genetic variation (Siol & al. 2008). Consequently, reliance on a single or a few loci may obscure true evolutionary divergence among closely related selfing species.

Modern genome-wide approaches such as RADseq or Hyb-Seq provide far greater resolution and are increasingly necessary to uncover cryptic diversity and accurately reconstruct species boundaries in selfing *Medicago* taxa (Branca & al. 2011; Yoder & al. 2013).

While anatomical and palynological characters are valuable for assessing plant diversity, they often exhibit plasticity and convergence, which limit their reliability in resolving relationships among closely related taxa. Environmental factors, parallel evolution, and homoplasy can obscure true phylogenetic signals in these traits (Endress 1994; Punt & al. 2007). As a result, anatomical and palynological data alone rarely provide definitive taxonomic conclusions and must be supplemented with robust molecular and detailed morphological datasets to achieve accurate species delimitation (Scotland & al. 2003; Soltis & Soltis 2000). The integration of multiple independent data sources is now considered essential for unraveling complex evolutionary histories and avoiding misleading classifications.

Resolving relationships among closely related taxa, particularly in groups with recent divergence and selfing mating systems like *Medicago*, requires a multifaceted approach. In this study, we combined molecular data (ITS and ETS), morphological, palynological, and anatomical analyses to clarify taxonomic boundaries between *M. rigidula*, *M. rigiduloides*, and their close relatives *M. constricta* and *M. sinskiae*.

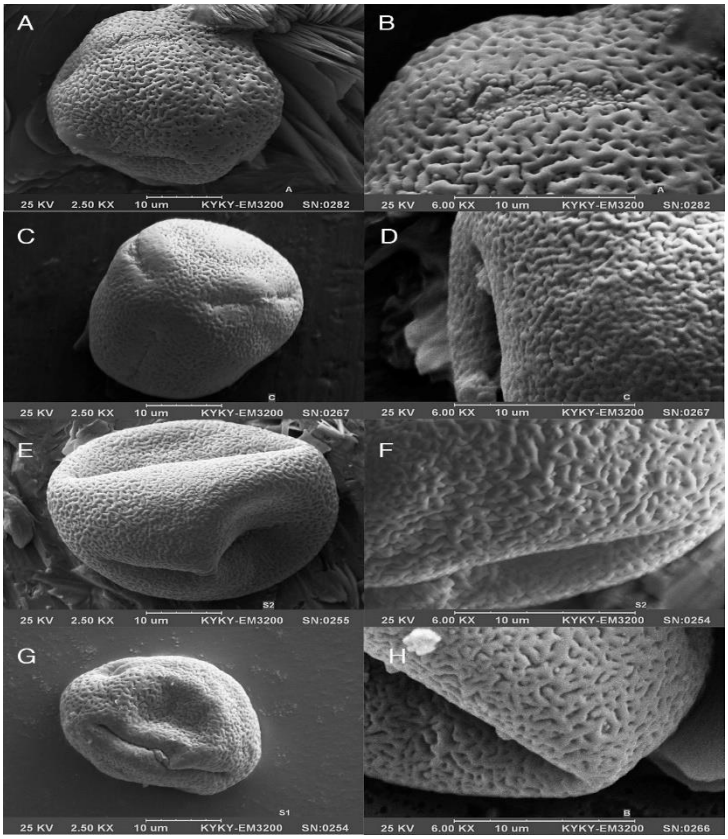

Fig. 5. SEM micrographs of pollen grains from different species of the *M. rigidula* complex: A–B: *M. constricta*; C–D: *M. rigidula*; E–F: *M. rigiduloides*; G–H: *M. sinskiae*.

Reliance on single markers often fails to reflect the complex evolutionary histories in selfing species, where limited gene flow and high genetic drift blur lineage distinctions (Ronfort & al. 2006; Yoder & al. 2013). By integrating nuclear markers (ITS, ETS) with phenotypic traits, we provided a more robust and comprehensive framework for species delimitation, reducing risks of misinterpretation caused by incomplete lineage sorting, hybridization, or morphological convergence (Branca & al. 2011; Greene & al. 2020).

As part of improving resolution within the core *Medicago* group, we designed a new pair of ETS primers specifically optimized for this lineage. Previous ETS primers showed variable amplification success in *Medicago* and related genera, limiting their usefulness in fine-scale phylogenetic analyses (Yoder & al. 2013). Our newly developed ETS primers consistently amplified target regions across multiple species in the core *Medicago* clade, providing a valuable tool for future molecular systematics and evolutionary research. The combination of multilocus molecular approaches with detailed morphological and anatomical studies thus represents a powerful strategy for uncovering the true evolutionary relationships in complex and rapidly evolving plant groups like *Medicago*.

Provisional key to the *M. rigidula* complex

Here, an identification key was created to provisionally identify newly collected material employed here for molecular and confirmatory morphological analyses. For full descriptions, please see Mehregan & Small (2023).

1. No gaps evident between coils of mature pod (sometimes coils so strongly adpressed their limits are not distinguishable); mature pods glabrous; curving veins at periphery of pod face almost concentric, little anastomosed ..... *M. constricta*

- Some gaps evident between coils of mature pods; mature pods usually velvety-glandular (with short gland-tipped hairs); radial veins strongly curved or S-shaped, sometimes anastomosed peripherally 2

2. Fruit short-cylindrical; radial veins moderately curved, strongly branched ..... *M. sinskiae*
- Fruit discoid, barrel-like, ovoid or spherical; radial veins on coil face strongly curved, moderately branched 3

3. Spine tips often strongly curved; pods often with up to 5 coils ..... *M. rigidula*
- Spine tips usually not strongly curved; pods often with more than 5 coils ..... *M. rigiduloides*

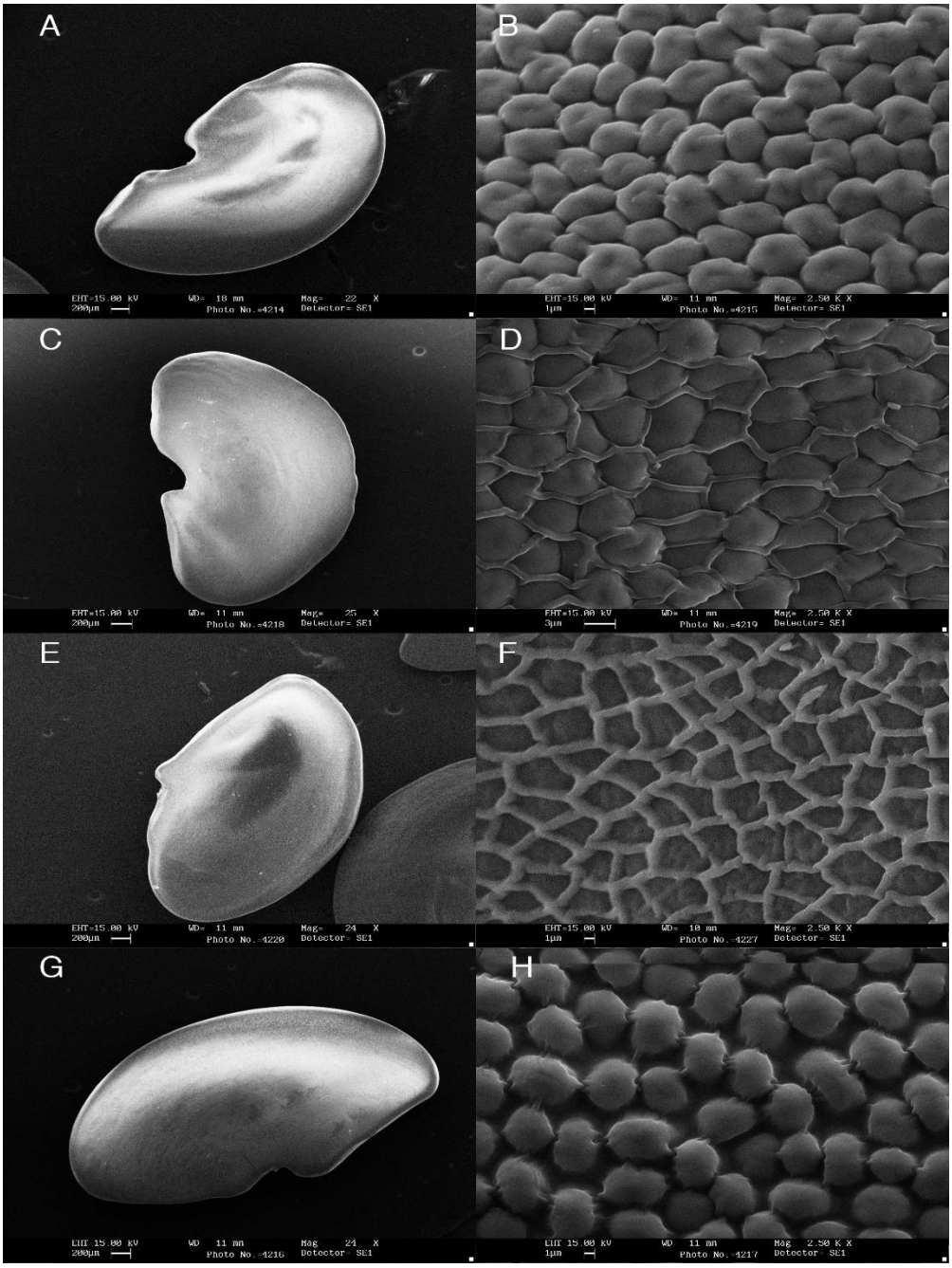

Fig. 6. SEM micrographs of seeds from different species of the *M. rigidula* complex: A–B: *M. constricta*; C–D: *M. rigidula*; E–F: *M. rigiduloides*; G–H: *M. sinskiae*.

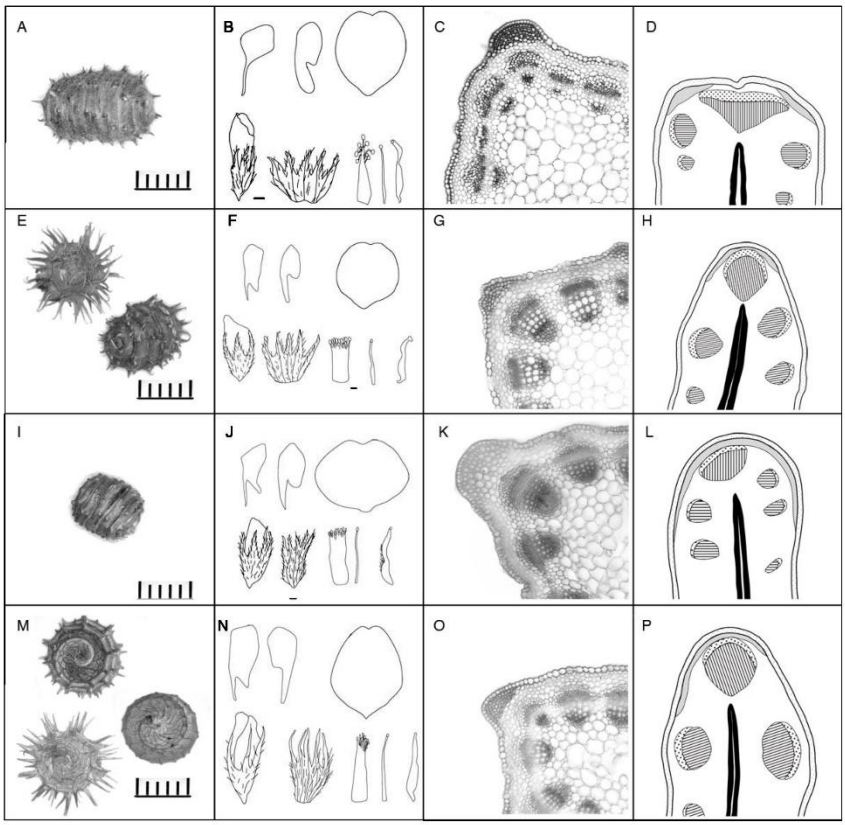

Fig. 7. Comparative images of pod (A, E, I, M) and flower (B, F, J, N; scale bar = 1 mm) morphology, and stem (C, G, K, O) and pod (D, H, L, P) anatomy in different species of the *M. rigidula* complex. A–D: *M. constricta*; E–H: *M. rigidula*; I–L: *M. rigiduloides*; M–P: *M. sinskiae*.

Taxonomy and distribution

1. *M. constricta* Durieu, Actes Soc. Linn. Bordeaux 29: 15 (1873).

Syn.: *M. rigidula* subsp. *constricta* (Durieu) Ponert, Feddes Repert. 83(9-10): 640 (1973); *M. globosa* sensu Urb. In Verh. Bot. Ver. Brandenb. 15: 71 (1873) et auct., non Persl (1822).

Distribution: Eastern Mediterranean area, Iraq, Iran (Luristan, Kohgilouyeh & Boyer-Ahmad, Fars, Khuzistan).

2. *M. sinskiae* Uljanova, Novosti Sist. Vyssh. Rast. 1: 175 (1964).

Syn.: *M. rigidula* subsp. *sinskiae* (Uljanova) Mehregan & Rahimin., Iran. J. Bot. 9(2): 214 (2002).

Distribution: Turkmenistan, Iran (Kurdistan, Luristan, Kohgilouyeh & Boyer-Ahmad).

3. *M. rigidula* (L.) All., Fl. Pedem. 1: 316 (1785).

Syn.: *M. polymorpha* L. κ *rigidula* L., Sp. Pl. 780 (1753); *M. polymorpha* L. μ *muricata* L., Sp. Pl. 781 (1753); *M. gerardii* Waldst. & Kit ex Willd., Sp. Pl., ed. 4 [Willdenow] 3(2): 1415 (1802); *M. agrestis* Ten., Fl. Nap. Prod. 45; et Cat. 59; Prod. Suppl. ii. p. lxxi. (1811-1815); *M. rigidula* subsp. *agrestis* (Ten.) Rouy in Rouy & Fouc., Fl. Fr. 5: 27 (1899); *M. rigidula* subsp. *cinerescens* (Jord.) Ponert, Feddes Repert. 83(9-10): 639 (1973).

Distribution: Europe, Turkey, Caucasus, Iran (Azerbaijan, Gilan, Mazandaran).

4. *M. rigiduloides* E.Small, Canad. J. Bot. 68(12): 2614 (1990).

Syn.: *M. rigidula* (L.) All. var. *submitis* Boiss., Fl. Orient. 2: 101 (1872).

Distribution: Europe, Turkey, Caucasus, Middle East, including Iran (all over the country except for the East and South-East)

ACKNOWLEDGEMENTS

The authors would like to thank M. Mahmoudi Shamsabad for her help in the preparation of the manuscript.

REFERENCES

Allioni, C. 1785: Flora Pedemontana sive Enumeratio Methodica Stirpium Indigenarum Pedemontii (Vol. 1). J. M. Briolus. -Turin, J.M. Briolus.

Azizian, D., & Cutler, D.F. 1982: Anatomical, cytological and phytochemical studies on *Phlomis* L. and Eremostachys Bunge (Labiatae). -Bot. J. Linn. Soc. 85(4): 249–281. https://doi.org/10.1111/j.1095-8339.1982.tb00373.x

Baldwin, B.G., & Markos, S. 1998: Phylogenetic utility of the external transcribed spacer (ETS) of 18S-26S rDNA: Congruence of ETS and ITS trees of *Calycadenia* (Compositae). -Mol. Phylogenet. Evol. 10(3): 449–463. https://doi.org/10.1006/mpev.1998.0545

Bayat, M., Assadi, M., Small, E., & Mehregan, I. 2021a: Investigating the taxonomic relationships and geographical distribution range of *Medicago rigidula* and *M. rigiduloides* in Iran. -Iran. J. Bot. 27(2): 115–129. https://doi.org/10.22092/ijb.2021.354838.1328

Bayat, M., Assadi, M., Small, E., & Mehregan, I. 2021b: Molecular studies of Iranian populations support the morphology-based taxonomic separation of *Medicago rigidula* and *M. rigiduloides*. -Phytotaxa 518(4): 281–299. https://doi.org/10.11646/phytotaxa.518.4.5

Bena, G. 2001: Molecular phylogeny supports the morphologically based taxonomic transfer of the "medicagoid" *Trigonella* species to the genus *Medicago* L. -Amer. J. Bot. 88(3): 466–475. https://doi.org/10.2307/2657114

Bena, G., Jubier, M.F., Olivieri, I., & Lejeune, B. 1998a: Ribosomal external and internal transcribed spacers: Combined use in the phylogenetic analysis of *Medicago* (Leguminosae). -J. Mol. Evol. 46(3): 299–306. https://doi.org/10.1007/pl00006306

Bena, G., Lejeune, B., Prosperi, J.M., & Olivieri, I. 1998b: Molecular phylogenetic approach for studying life-history evolution: The ambiguous example of the genus *Medicago* L. -Proc. Roy. Soc. B: Biol. Sci. 265(1401): 1141–1151. https://doi.org/10.1098/rspb.1998.0410

Bena, G., Prosperi, J.M., Lejeune, B., & Olivieri, I. 1998c: Evolution of annual species of the genus *Medicago*: A molecular phylogenetic approach. -Mol. Phylogenet. Evol. 9(3): 552–559. https://doi.org/10.1006/mpev.1998.0493

Branca, A., Paape, T., Zhou, P., Briskine, R., Farmer, A.D., Mudge, J., ... & Young, N.D. 2011: Whole-genome nucleotide diversity, recombination, and linkage disequilibrium in the model legume *Medicago truncatula*. -Proc. Natl. Acad. Sci. 108(42): E864–E870. https://doi.org/10.1073/pnas.1104032108

Douzery, E.J.P., Pridgeon, A.M., Kores, P., Linder, H. P., Kurzweil, H., & Chase, M.W. 1999: Molecular phylogenetics of *Diseae* (Orchidaceae): a contribution from nuclear ribosomal ITS sequences. -Amer. J. Bot. 86(6): 887–899. https://doi.org/10.2307/2656709

Downie, S.R., Katz-Downie, D.S., Rogers, E.J., Zujewski, H.L., & Small, E. 1998: Multiple independent losses of the plastid rpoC1 intron in *Medicago* (Fabaceae) as inferred from phylogenetic analyses of nuclear ribosomal DNA internal transcribed spacer sequences. –Can. J. Bot. 76(5): 791–803. https://doi.org/10.1139/b98-056

Doyle, J. J., & Doyle, J. L. 1987: A rapid DNA isolation procedure for small quantities of fresh leaf tissue. -Phytochem. Bull. 19: 11–15.

Endress, P.K. 1994: Diversity and evolutionary biology of tropical flowers. Cambridge University Press. -Cambridge, Cambridge University Press.

Erdtman, G. 1960: Pollen walls and angiosperm phylogeny. -Bot. Not. 113: 41–45.

Felsenstein, J. 1988: Phylogenies from molecular sequences: Inference and reliability. -Ann. Rev. Genet. 22: 521–565. https://doi.org/10.1146/annurev.ge.22.120188.002513

Greene, S. L., Kisha, T. J., & Yu, L. X. 2020: Genetic diversity and population structure of *Medicago* species in relation to their center of diversity. -Crop Sci. 60(6): 3152–3164. https://doi.org/10.1002/csc2.20265

Heyn, C.C. 1963: The annual species of *s*. -Jerusalem, Magnes Press, The Hebrew University.

Heyn, C.C. 1970: *Medicago* [annuals]. In P. H. Davis (Ed.), Flora of Turkey and the East Aegean Islands (Vol. 3, pp. 494–510). Edinburgh University Press. -Edinburgh, Edinburgh University Press.

Heyn, C.C. 1984: *Medicago*. In K.H. Rechinger (Ed.), Flora Iranica (Vol. 157, Papilionaceae II, pp. 253–274). Akademische Druck- u. Verlagsanstalt. -Graz, Akademische Druck- u. Verlagsanstalt.

Linnaeus, C. 1753: Species Plantarum (Vol. 2). Impensis Laurentii Salvii. -Stockholm, Impensis Laurentii Salvii.

Maddison, D.R., & Maddison, W.P. 2005: MacClade 4: Analysis of phylogeny and character evolution. Version 4.08a. Sinauer Associates. -Sunderland, Sinauer Associates.

Maureira-Butler, I.J., Pfeil, B.E., Muangprom, A., Osborn, T.C., & Doyle, J.J. 2008: The reticulate history of *Medicago* (Fabaceae). -Syst. Biol. 57(3):

466–482. https://doi.org/10.1080/10635150802172168

Mehregan, I., Rahiminejad, M.R., & Azizian, D. 2002: A taxonomic revision of the genus *Medicago* L. (Fabaceae) in Iran. -Iran. J. Bot. 9(2): 207–221.

Mehregan, I. & Small, E. 2023: The genus *Medicago* L. In: M. Assadi & A.A. Maassoumi (eds.). Flora of Iran no. 177: 261-364.

Miller, P. 1768: The Gardeners' Dictionary (8th ed.). Printed for the author. -London, Printed for the author.

Posada, D., & Crandall, K. A. 1998: Modeltest: Testing the model of DNA substitution. -Bioinformatics 14(9): 817–818. https://doi.org/10.1093/bioinformatics/14.9.817

Punt, W., Hoen, P. P., Blackmore, S., Nilsson, S., & Le Thomas, A. 2007: Glossary of pollen and spore terminology. -Rev. Palaeobot. Palynol. 143(1–2): 1–81. https://doi.org/10.1016/j.revpalbo.2006.06.008

Ronfort, J., Bataillon, T., Santoni, S., Delalande, M., David, J. L., & Prosperi, J. M. 2006: Microsatellite diversity and broad scale geographic structure in a selfing species: *Medicago truncatula*. -Genetics 172(1): 373–386. https://doi.org/10.1534/genetics.105.044354

Ronquist, F., Huelsenbeck, J.P., & Van der Mark, P. 2005: MrBayes 3.1 Manual. Draft 5/17/2005.

Shaffer, H.B., & Thomson, R.C. 2007: Delimiting species in recent radiations. -Syst. Biol. 56(6): 896–906. https://doi.org/10.1080/10635150701772563

Scotland, R.W., Olmstead, R.G., & Bennett, J. R. 2003: Phylogeny reconstruction: the role of morphology. -Syst. Biol. 52(4): 539–548. https://doi.org/10.1080/10635150390223620

Siol, M., Prosperi, J. M., Bonnin, I., & Ronfort, J. 2008: How multilocus genotypic pattern helps to understand the history of selfing populations: A case study in *Medicago truncatula*. -Heredity 100(6): 517–525. https://doi.org/10.1038/hdy.2008.7

Small, E. 1987a: A taxonomic study of the "medicagoid" *Trigonella* (Leguminosae). -Can. J. Bot. 65(6): 1199–1211. https://doi.org/10.1139/b87-166

Small, E. 1990: *Medicago rigiduloides*, a new species segregated from *M. rigidula*. -Can. J. Bot. 68(12): 2614–2617. https://doi.org/10.1139/b90-330

Small, E., Brookes, B. & Crawford, E.J. 1990: Intercontinental differentiation in *Medicago rigidula*. –Can. J. Bot. 68: 2607-2613.

Small, E. 2011: Alfalfa and relatives: Evolution and classification of *Medicago*. NRC Research Press. -Ottawa, NRC Research Press.

Small, E., & Jomphe, M. 1989: A synopsis of the genus *Medicago* (Leguminosae). -Can. J. Bot. 67(11): 3260–3294. https://doi.org/10.1139/b89-405

Small, E., Lassen, P., & Brookes, B.S. 1987: An expanded circumscription of *Medicago* (Leguminosae, Trifolieae) based on explosive flower tripping. -Willdenowia 16(2): 415–437.

Soltis, D.E., & Soltis, P.S. 2000: Contributions of plant molecular systematics to studies of molecular evolution. -Plant Mol. Biol. 42(1): 45–75. https://doi.org/10.1023/A:1006380618351

Steele, K. P., & Wojciechowski, M. F. 2003: Phylogenetic analyses of tribes Trifolieae and Vicieae, based on sequences of the plastid gene, matK (Papilionoideae: Leguminosae). In B.B. Klitgaard & A. Bruneau (Eds.), Advances in legume systematics (Part 10, pp. 355–370). Royal Botanic Gardens, Kew. -Kew, Royal Botanic Gardens.

Steele, K.P., Ickert-Bond, S.M., Zarre, S., & Wojciechowski, M.F. 2010: Phylogeny and character evolution in *Medicago* (Leguminosae): Evidence from analyses of plastid trnK/matK and nuclear GA3ox1 sequences. -Amer. J. Bot. 97(7): 1142–1155. https://doi.org/10.3732/ajb.1000009

Swofford, D.L. 2002: PAUP: Phylogenetic analysis using parsimony* (and other methods). Version 4. Sinauer Associates. -Sunderland, Sinauer Associates.

Wojciechowski, M.F., Lavin, M., & Sanderson, M. J. 2003: A phylogeny of legumes based on sequences of the plastid matK gene. In Botany 2003: Aquatic and Wetland Plants: Wet and Wild, Abstracts (p. 99).

Wojciechowski, M.F., Lavin, M., & Sanderson, M.J. 2004: A phylogeny of legumes (Leguminosae) based on analysis of the plastid matK gene resolves many well-supported subclades within the family. Am. J. Bot, 91(11): 1846–1862. https://doi.org/10.3732/ajb.91.11.1846

Yoder, J.B., Briskine, R., Mudge, J., Farmer, A., Paape, T., Steele, K., & Young, N. D. 2013: Phylogenomic analysis of *Medicago* species reveals clear species boundaries and evidence of reticulate evolution. -BMC Evol. Biol. 13, 131. https://doi.org/10.1186/1471-2148-13-131

Zareei, R., Small, E., Assadi, M., Mehregan, I. 2022: Genetic structure of *Medicago sinskiae* using microsatellite data reveals its fast expansion throughout western and southwestern Iran. -Collect. Bot. 41: e2002. https://doi.org//10.3989/collectbot.2022.v41.002

Appendix 1. Accession number of taxa previously published on GenBank (ETS, ITS2, and ITS1, respectively).

M. arabica (L.) Huds., Z97705, Z97680, Z97655; *M. arborea* L., Z99239, Z99223, Z99207; *M. bonarotiana* Arcang., Z99240, Z99224, Z99208; *M. cancellata* M. Bieb., Z99241, Z99225, Z99209; *M. carstiensis* Wulf., Z99242, Z99226, Z99210; *M. ciliaris* (L.) Krocker., Z97706, Z97681, Z97656; *M. constricta* Durieu., Z92938, Z92925, Z92912; *M. disciformis* DC., Z97708, Z97682, Z97657; *M. doliata* Carmign., Z92939, Z92926, Z92913; *M. edgeworthii* Sirjaev., AY256404, AF028438, AF028378; *M. falcata* L., Z99245, Z99229, Z99213; *M. glomerata* Balb., Z99246, Z99230, Z99214; *M. granadensis* Willd., Z97710, Z97683, Z97658; *M. heyniana* Greuter., Z97711, Z97684, Z97659; *M. hybrida* (Pourr.) Trautv., Z99247, Z99231, Z99215; *M. intertexta* (L.) Miller., Z97712, Z97685, Z97660; *M. laciniata* (L.) Miller., Z97714, Z97686, Z97661; *M. lanigera* E. Winkl. & B. Fedtsch., AY256405, AF028445, AF028385; *M. littoralis* Rohde ex Loisel., Z92940, Z92927, Z92914; *M. lupulina* L., Z99248, Z99232, Z99216; *M. marina* L., Z99249, Z99233, Z99217; *M. medicaginoides* (Retz.) E. Small., AY256406, AF028450, AF028390; *M. minima* (L.) Bart., Z97715, Z97689, Z97664; *M. monantha* (C.A. Meyer) Trautv., AY256407, AF028453, AF028393; *M. monspeliaca* (L.) Trautv., AY256408, AF028452, AF028392; *M. murex* Willd., Z92941, Z92928, Z92915; *M. muricoleptis* Tin., Z97716, Z97690, Z97665; *M. noeana* Boiss., Z92942, Z92929, Z92916; *M. orbicularis* (L.) Bart., Z97718, Z97691, Z97666; *M. pironae* Vis., Z99250, Z99234, Z99218; *M. polyceratia* (L.) Trautv., AY256410, AF028461, AF028401; *M. polymorpha* L., Z92943, Z92930, Z92917; *M. popovii* (Korovin) Sirj., AY256411, AY256400, AY256400; *M. praecox* DC., Z92944, Z92931, Z92918; *M. radiata* L., Z92945, Z92932, Z92919; *M. rigidula* (L.) All., Z92946, Z92933, Z92920; *M. rigiduloides* E. Small., Z99251, Z99235, Z99219; *M. rotate* Boiss., Z92947, Z92934, Z92921; *M. rugosa* Desr., Z97719, Z97692, Z97667; *M. ruthenica* (L.) Trautv., AY256413, AF028414, AF028354; *M. sativa* L., AY256403, Z99236, Z99220; *M. sauvagei* Negre., Z97720, Z97693, Z97668; *M. scutellata* (L.) Miller., Z97721, Z97694, Z97669; *M. secundiflora* Durieu., Z97722, Z97695, Z97670; *M. shepardii* Post ex Boiss., Z97723, Z97697, Z97671; *M. soleirolii* Duby., Z97724, Z97698, Z97672; *M. suffruticosa* Ramond ex DC., Z99253, Z99237, Z99221; *M. syriaca* E. Small., Z97727, Z97699, Z97674; *M. tenoreana* Ser., Z99254, AF028472, AF028412; *M. truncatula* Gaertn., Z92949, Z92936, Z92923; *Trifolium pretense* L., Z97729, EU348780, AF053171; *Melilotus italica* Lam., Z97713, Z97688, Z97663; *Trigonella cretica* Boiss., Z97707, JX274209, JX274208.